

Taming flavour violation in the Inverse Seesaw

Jonathan Kriewald ^a and Ana M. Teixeira ^b

^a Jožef Stefan Institut, Jamova Cesta 39, P. O. Box 3000, 1001 Ljubljana, Slovenia

^b Laboratoire de Physique de Clermont Auvergne (UMR 6533), CNRS/IN2P3, Univ. Clermont Auvergne, 4 Av. Blaise Pascal, 63178 Aubière Cedex, France

Abstract

The Inverse Seesaw mechanism remains one of the most attractive explanations for the lightness of neutrino masses, allowing for natural low-scale realisations. We consider the prospects of a simple extension via 3 generations of sterile fermions - the so called ISS(3,3) - in what concerns numerous lepton flavour observables. In order to facilitate a connection between the Lagrangian parameters and low-energy data, we systematically develop new parametrisations of the Yukawa couplings. Relying on these new parametrisations to explore the parameter space, we discuss the complementary role of charged lepton flavour violation searches in dedicated facilities, as well as in lepton colliders (FCC-ee and μ TRISTAN). Our results reveal the strong synergy of the different indirect searches in probing the distinct flavour sectors of the model. In particular, we show that in the absence of radiative decays $\ell_\alpha \rightarrow \ell_\beta \gamma$, sizeable rates for Z -penguin dominated observables could hint at a non-trivially mixed and non-degenerate heavy spectrum.

1 Introduction

Oscillation data (i.e. the smallness of neutrino masses and the pattern of leptonic mixings) remains one of the most pressing open issues in particle physics, signalling a clear departure from the Standard Model (SM). Among the numerous New Physics (NP) models which have been put forward to address the problem of neutrino mass generation, certain constructions offer the appealing possibility of being realised at low-energies, opening the door to direct searches for the new resonances, and/or to indirect signals. The latter emerge as a consequence of new contributions to both SM-like observables (including for example electroweak precision tests) and to SM-forbidden processes (as is the case of charged lepton flavour violation transitions and decays).

The Inverse Seesaw mechanism (ISS) [1–3] consists in a variant of the type I Seesaw [4–8], in which two species of sterile fermions are added to the SM particle content, X and ν_R . The relevant terms in the Lagrangian are given by

$$\mathcal{L}_{\text{ISS}} = -Y_{ij}^D \bar{L}_i^c \tilde{H} \nu_{Rj}^c - M_R^{ij} \bar{\nu}_{Ri} X_j - \frac{1}{2} \mu_R^{ij} \bar{\nu}_{Ri}^c \nu_{Rj} - \frac{1}{2} \mu_X^{ij} \bar{X}_i^c X_j + \text{H.c.} . \quad (1)$$

From this Lagrangian, the mass matrix of the neutral fermions in the basis (ν_L, ν_R^c, X) can be cast as

$$M_{\text{ISS}} = \begin{pmatrix} 0 & m_D & 0 \\ m_D^T & \mu_R & M_R \\ 0 & M_R^T & \mu_X \end{pmatrix} , \quad (2)$$

with $m_D = v Y_D / \sqrt{2}$, in which v denotes the electroweak (EW) vacuum expectation value. By setting $\mu_{X,R} \rightarrow 0$, one recovers total lepton number conservation as a global symmetry of the Lagrangian in Eq. (1), and having small $\mu_{X,R}$ becomes technically natural in the sense of 't Hooft [9, 10]. In the

limit of small $\mu_{X,R} \ll m_D \ll M_R$, one can thus perturbatively (block-)diagonalise the mass matrix in Eq. (2) and obtain to leading order

$$m_\nu \simeq m_D (M_R^{-1})^T \mu_X M_R^{-1} m_D^T \equiv U_{\text{PMNS}}^* m_\nu^{\text{diag}} U_{\text{PMNS}}^\dagger, \quad (3)$$

for the light neutrino masses. The mass spectrum of the heavy sterile states is instead strongly restricted, since these combine to form approximately degenerate pseudo-Dirac pairs, as a consequence of the small lepton number breaking via μ_X (with the mass splittings proportional to μ_X). Notice that the Majorana mass term μ_R is absent from Eq. (3), as it only appears in higher orders in the seesaw expansion (and in loop corrections to the neutrino mass matrix [11]); thus, in the interest of simplicity it will be henceforth neglected. In what follows we will consider a ‘‘symmetric’’ realisation of the ISS in which $n_R = n_X = 3$ generations of heavy sterile fermions are added to the SM particle content, the so-called ISS(3,3)¹, leading to square matrices μ_X, M_R, m_D .

Due to the ‘‘double-suppression’’ of simultaneously having a large M_R and a small μ_X , the mass scale of the physical heavy states can be lowered to the TeV-scale while retaining $\mathcal{O}(1)$ Yukawa couplings. Thus, the ISS can have a very rich phenomenology with potentially sizeable contributions to a plethora of low-energy (flavour) observables [12–19], (precision) observables at the Z -pole [20–23] as well as potentially detectable collider signatures [24–26]. Consequently, it is desirable to have a clear connection between the Lagrangian parameters and low-energy data, and ideally express them in terms of masses and mixings which can be related to physical observables.

A first attempt can be made relying on a modified Casas-Ibarra parametrisation [27], which allows to directly incorporate neutrino oscillation data into the Yukawa couplings by means of the Pontecorvo-Maki-Nakagawa-Sakata (PMNS) matrix and the measured atmospheric and solar mass squared differences. However, as we proceed to point out, the connection to other low-energy data such as various lepton universality tests, proves to be rather difficult due to the non-linear nature of the involved matrix equations. Here, we systematically develop alternative parametrisations that directly encode low-energy data from universality tests and oscillation data into the Yukawa couplings and (Majorana) mass matrices. We further demonstrate their usefulness in disentangling distinct sources of flavour violation, that is flavour-violation from active-sterile mixing, and from mixings exclusively amongst the heavy states. This is done through a dedicated phenomenological analysis of various low-energy charged lepton flavour violation (cLFV) observables, cLFV and lepton flavour universality violation (LFUV) Z -pole observables, as well as the potential impact of cLFV searches at a μ^+e^- (μ TRISTAN) collider.

The remainder of the manuscript is organised as follows. In Section 2, we systematically develop new parametrisations of the ISS(3,3) from simple algebraic arguments. In Section 3 we describe the observables and their experimental status, which will be used in the phenomenological analysis of Section 4. We finally conclude in Section 5.

2 Parametrising the ISS(3,3): incorporating low-energy data

As mentioned before, a low-energy mechanism of neutrino mass generation as the ISS is expected to lead to abundant contributions to flavoured observables and to EW precision probes. In order to explore the flavour content of such classes of models, phenomenological studies frequently rely on parametrisations of the flavour structures of the model (which typically ensure that neutrino oscillation data is accommodated).

As a possible first approach to study the phenomenology of the ISS, one can begin by considering a modified Casas-Ibarra parametrisation [27],

$$v Y_D^T = m_D^T = V^\dagger \sqrt{M^{\text{diag}}} R \sqrt{m_\nu^{\text{diag}}} U_{\text{PMNS}}^\dagger. \quad (4)$$

In the above, the Yukawa couplings encode neutrino data, with a complex orthogonal matrix, R , parametrising the additional degrees of freedom. Moreover, in Eq. (4) the unitary matrix V diagonalises $M = V^\dagger M^{\text{diag}} V^*$ with $M = M_R \mu_X^{-1} M_R^T$.

¹For a detailed discussion of the most minimal ISS realisations, see [12].

While the Casas-Ibarra parametrisation allows for a simple (and for the most part numerically stable) access to the ISS(3,3) parameter space that is consistent with neutrino oscillation data, it has significant drawbacks. Firstly, the “ R -matrix” has no direct physical interpretation, thus leading to ambiguities which cannot be easily resolved. Secondly, an arbitrary complex *orthogonal* matrix - as R - is parametrised via 3 Euler rotations, which naturally leads to a hyperbolic dependence on the imaginary parts of the mixing angles. In turn, this can translate into a poor behaviour of the numerical sampling of the parameter space, as one quickly runs into non-perturbative regimes (see e.g. [28] for attempts to cure this behaviour). Finally, due to the “entanglement” of the PMNS and R -matrix flavour structures in m_D (cf. Eq. (4)), it becomes very hard (if not impossible) to disentangle different directions in “flavour-violation-space”. It further renders complying with broad classes of low-energy data (cLFV, EW, LFUV, ...) a complicated and not very transparent exercise.

As originally proposed in [29], the deviations from unitarity of the 3×3 would-be PMNS block of the unitary leptonic mixing matrix offer a convenient means of encoding the constraints from low-energy data. The so-called “ η -matrix” is defined as

$$U_{\text{PMNS}} \rightarrow \tilde{U}_{\text{PMNS}} = (\mathbb{1} - \eta) U_{\text{PMNS}}. \quad (5)$$

Perturbatively diagonalising the ISS(3,3) mass matrix, one can derive an approximate expression for η as

$$\eta \simeq \frac{1}{2} m_D^* (M_R^{-1})^\dagger (M_R^{-1}) m_D^T. \quad (6)$$

It is important to notice that after integrating out the new heavy degrees of freedom, the deviation from unitarity induces a potentially lepton flavour (universality) violating $d = 6$ operator at tree-level [30, 31]

$$\mathcal{L}_{d=6} = \frac{i}{2} \eta_{\alpha\beta} \left[(\bar{L}_\alpha \gamma_\mu L_\beta) (\phi^\dagger \overleftrightarrow{D}_\mu \phi) - (\bar{L}_\alpha \gamma_\mu \tau^i L_\beta) (\phi^\dagger \overleftrightarrow{D}_\mu^i \phi) \right]. \quad (7)$$

In view of this brief discussion, it becomes desirable to have a parametrisation of the neutrino mass matrix that allows for a calculable connection between the Lagrangian parameters and low-energy data beyond neutrino oscillations. In what follows, we will explore several possible avenues to do so, describing the underlying algebraic approach, as well as the most relevant phenomenological consequences.

Let us first notice that inserting the Casas-Ibarra parametrisation for m_D into the definition of η , and subsequently inverting R might be technically possible but is highly impractical. Another possibility would be to reverse-engineer a parametrisation for M_R that would allow controlling the “non-unitarity” of \tilde{U}_{PMNS} ; nonetheless, this would imply losing control of the heavy mass scale (M_R), which would also be impractical from a phenomenologist’s point of view (especially if one desires to infer information on the scale of NP from low-energy data). In the case of invertible M_R and m_D , an alternative parametrisation has been put forward in [32] (see also [33] and [23] for modified versions), in which oscillation data is encoded in the lepton number violating term μ_X rather than in m_D . Considering here the ISS(3,3), for any invertible M_R and m_D one can then write

$$\mu_X = M_R^T m_D^{(-1)} U_{\text{PMNS}}^* \text{diag}(m_{\nu_1}, m_{\nu_2}, m_{\nu_3}) U_{\text{PMNS}}^\dagger (m_D^T)^{(-1)} M_R. \quad (8)$$

In principle, this allows retaining full control over the heavy mass scale and the flavour structure of m_D , while the Majorana mass μ_X becomes intrinsically related to the scale of the active neutrino masses. This is, from a phenomenologist’s point of view, a very useful approach to *systematically* explore low-energy implications of the ISS. Although the only condition on M_R is that it be invertible, for the purpose of this work we will focus our attention on possible flavour structures of m_D .

In [32] and [34] the authors propose to reverse-engineer textures for m_D which are expected to lead to maximal effects (e.g. cLFV) along certain “flavoured-directions”: for instance, aiming at maximising $\mu\tau$ -flavour violating observables while evading the strong constraints stemming from $e - \mu$ sector flavour observables. For this purpose, it was proposed to construct fixed textures for m_D , only varying an overall factor; likewise, the heavy masses are taken to be degenerate, and the mass scale

M_R is only varied through an overall factor. The parametrisation of m_D (where m_D is for simplicity assumed to be real) used in [32, 34] is thus given by

$$m_D = v A \cdot \mathcal{O}, \quad (9)$$

where A is an invertible lower triangular matrix and \mathcal{O} a real orthogonal matrix. Notice that should M_R be diagonal and universal, then \mathcal{O} trivially disappears from the expression of η (cf. Eq. (6)), and does not contribute to flavour violation in this minimal scenario. The texture of A is then chosen to optimally explore certain flavoured configurations (such as the example mentioned above - i.e., maximising flavour violation in the $e\tau$ and $\mu\tau$ directions, while strongly suppressing $e\mu$ transitions).

The authors of [33] further notice that it can be useful to re-scale m_D with M_R/v , so that one parametrises the active-sterile mixing rather than the Yukawa couplings. This was further exploited in [23], where the goal was to find regions of the parameter space which allowed maximising lepton flavour universality violation while retaining control over lepton flavour violation. The desired features can be automatically ensured by parametrising m_D as follows

$$m_D = \text{diag}(y_1, y_2, y_3) \cdot \mathcal{V} \cdot M_R^T, \quad (10)$$

in which \mathcal{V} is a unitary matrix. Upon insertion of this parametrisation in Eq.(6) one is readily led to

$$\eta = \text{diag}(y_1^2, y_2^2, y_3^2), \quad (11)$$

so that flavour violation can only appear via a non-trivial \mathcal{V} , and only in the case of non-degenerate eigenvalues of M_R . Furthermore, constraints from low-energy data can be trivially incorporated by appropriately fixing y_i .

In the present study we aim at generalising the work that has been done in [23, 32–34], with the goal of disentangling PMNS (i.e. oscillation data) from additional beyond the SM (BSM) sources of flavour violation, relying on a simple algebraic approach (using the properties of invertible square matrices). Throughout our discussion we will always focus on the ISS(3,3) realisation - even if not explicitly mentioned.

We begin by noticing that the only requirement on m_D is that it be invertible, i.e. that its determinant be different from 0. Any matrix has a polar decomposition, which is unique in the case of an invertible square matrix. We can thus write $Y_D = m_D/v$ in full generality as

$$Y_D^{\text{polar}} = P \cdot \mathcal{U}, \quad (12)$$

in which P is a positive definite hermitian matrix $P^\dagger = P$ and \mathcal{U} is unitary $\mathcal{U}^\dagger \mathcal{U} = \mathbb{1}$. The generally 9 complex (or equivalently 18 real) free parameters of m_D are encoded in 3 real angles and 6 phases in \mathcal{U} , 3 real diagonal elements of P , and 3+3 real parameters in the complex off-diagonal elements of P . Inserting this definition of Y_D into Eq. (6) (with the re-scaling of Y_D with M_R), one quickly finds

$$\eta = \frac{1}{2} P^* P^T, \quad (13)$$

such that P can now be written as

$$P = \sqrt{2} \eta^{\frac{1}{2}}, \quad (14)$$

where $\eta^{\frac{1}{2}}$ is a *hermitian* matrix square-root² of η . The matrix square-root can be found numerically through the Schur method or eigenvalue decomposition, or analytically with the help of the Cayley-Hamilton theorem, as recently derived in [35]. Following the eigenvalue decomposition, it is further clear that in order to ensure the invertibility of m_D , $\eta^{\frac{1}{2}}$ and therefore η have to be invertible (i.e. non-singular), which restricts the values η can take. Due to its phenomenological origin as a “deviation

²Via the eigenvalue decomposition one can easily show that all square roots of a positive definite hermitian matrix are also hermitian and positive definite.

from unitarity” of the PMNS matrix, the off-diagonal elements of η are not completely arbitrary and are subject to Schwarz inequalities given by [36, 37]

$$|\eta_{ij}| \leq \sqrt{\eta_{ii} \eta_{jj}}. \quad (15)$$

Notice that the off-diagonal elements of η can have complex phases; only their magnitudes are constrained by Eq. (15). In order to automatically comply with low-energy data we can parametrise η as

$$\eta = \begin{pmatrix} \eta_{ee} & \sqrt{\eta_{ee} \eta_{\mu\mu}} a \exp(i\delta_{12}) & \sqrt{\eta_{ee} \eta_{\tau\tau}} b \exp(i\delta_{13}) \\ \sqrt{\eta_{ee} \eta_{\mu\mu}} a \exp(-i\delta_{12}) & \eta_{\mu\mu} & \sqrt{\eta_{\mu\mu} \eta_{\tau\tau}} c \exp(i\delta_{23}) \\ \sqrt{\eta_{ee} \eta_{\tau\tau}} b \exp(-i\delta_{13}) & \sqrt{\eta_{\mu\mu} \eta_{\tau\tau}} c \exp(-i\delta_{23}) & \eta_{\tau\tau} \end{pmatrix}, \quad (16)$$

in which $0 < \eta_{ee, \mu\mu, \tau\tau} < 1$ and $0 \leq a, b, c < 1$. The non-singularity of $\eta^{\frac{1}{2}}$ allows deriving a further condition from the non-vanishing determinant as

$$\det \eta^{\frac{1}{2}} = \sqrt{\det \eta} = \sqrt{\eta_{ee} \eta_{\mu\mu} \eta_{\tau\tau} (1 - a^2 - b^2 - c^2 + 2abc \cos(\delta_{12} - \delta_{13} + \delta_{23}))} \neq 0. \quad (17)$$

The (diagonal) entries of η can then be fixed to the upper limits derived in global analyses as done in [37].

Alternatively, Y_D can be parametrised via the help of the QR decomposition: recall that any matrix A can be decomposed into a unitary matrix Q and an upper triangular matrix R as $A = QR$ and consequently into a lower triangular matrix as $A^\dagger = LQ^\dagger$ in which $L = R^\dagger$. Thus Y_D can be parametrised as

$$Y_D^{\text{QR}} = LU, \quad (18)$$

in which U is unitary and L is lower triangular, with $L_{ii} \neq 0$ (since Y_D must be invertible). Inserting this parametrisation into Eq. (6) (again together with the re-scaling of Y_D with M_R) one has

$$\eta = \frac{1}{2} L^* L^T, \quad (19)$$

and thus L can be found from the Cholesky decomposition of η (which is unique since η is positive definite). It is interesting to notice that this parametrisation corresponds exactly to what was found in [32, 34] in the limit of a real Y_D , see Eq. (9).

Both Y_D^{polar} and Y_D^{QR} parametrisations have the advantage that compliance with low-energy data in the form of bounds on η can be trivially encoded in Y_D . However, one still needs to compute the Cholesky decomposition or matrix square-root of η which can be analytically cumbersome. We detail in Appendix A the analytical Cholesky decomposition of a complex 3×3 matrix and refer to [35] for the analytical expression for the 8 matrix square-roots (and their inverses). Moreover, one can accidentally run into cases in which the condition of Eq. (17) is violated; setting the phases $\delta_{ij} = 0$ and $a = b = c = 1$ saturates the Schwarz inequalities of Eq. (15) and leads to a vanishing determinant, which in turn makes η singular and thus non-invertible. Additionally, having a small determinant (e.g. by setting a, b, c to a number slightly smaller than 1) can quickly become problematic for the numerical inversion of m_D , and lead to significant loss of precision.

A third option³ relies on a singular value decomposition (SVD) of Y_D . Any complex matrix A , in this case a complex square matrix, can be decomposed into

$$A = \mathcal{V}_1 \text{diag}(\sigma_1, \sigma_2, \dots, \sigma_n) \mathcal{V}_2^\dagger, \quad (20)$$

in which $\mathcal{V}_{1,2}$ are unitary matrices and σ_i are the singular values of A . Ensuring that A is non-singular (and thus invertible) conditions each of the singular values to be $\sigma_i \neq 0$. Consequently, the Yukawa couplings can be parametrised as

$$Y_D^{\text{SVD}} = \mathcal{V}_1 \text{diag}(y_1, y_2, y_3) \mathcal{V}_2^\dagger, \quad (21)$$

³One can also parametrise a general invertible square matrix via a LU decomposition, a Schur decomposition or an eigenvalue decomposition with complex eigenvalues. However, the connection of the involved matrices to physical observables is a priori much less clear than in the parametrisations proposed in this study, and thus we will not discuss them here.

in which $y_i > 0$ without loss of generality⁴. The unitary matrices can each be parametrised via 3 Euler angles, 3 “Dirac-like” phases δ_{ij} and 3 “Majorana-like” phases φ_i as

$$\mathcal{V}_{1,2} = O_{23} O_{13} O_{12} \text{diag}(e^{i\varphi_1}, e^{i\varphi_2}, e^{i\varphi_3}), \quad (22)$$

with O_{ij} given in the usual form; for example O_{23} can be given as

$$O_{23} = \begin{pmatrix} 1 & 0 & 0 \\ 0 & \cos \theta_{23} & \sin \theta_{23} e^{i\delta_{23}} \\ 0 & -\sin \theta_{23} e^{-i\delta_{23}} & \cos \theta_{23} \end{pmatrix}. \quad (23)$$

Notice that out of the 6 Majorana-like phases only 3 linear combinations are physical, as can be seen immediately upon insertion of \mathcal{V}_1 and \mathcal{V}_2 in Eq. (21). Further rescaling Y_D with M_R^T/v , and inserting it into Eq. (6) allows making the connection to low-energy data via

$$\eta = \frac{1}{2} \mathcal{V}_1^* \text{diag}(y_1^2, y_2^2, y_3^2) \mathcal{V}_1^T, \quad (24)$$

such that in the case of a trivial $\mathcal{V}_1 = \mathbb{1}$ one is trivially led to $y_i = \sqrt{2\eta_{ii}}$. Furthermore, one can relate \mathcal{V}_1 and y_i to the eigenvalue decomposition of η , for which the analytical expressions are in general very involved.

Notice that one can also fix y_i for the trivial case, and then vary the angles and phases of \mathcal{V}_1 for the purpose of dedicated numerical scans. In this case, the Schwartz inequality is automatically fulfilled, and in fact never saturated as long as $y_i > 0$. Furthermore, the angles θ_{ij} in \mathcal{V}_1 have a simple geometrical interpretation of directions in “flavour violation space”. In fact, \mathcal{V}_1 describes the flavour-violating mixing between active generations and the heavy states and leads to off-diagonal entries in η . In a similar fashion to what occurred in previous examples for the right-hand side unitary matrices, the matrix \mathcal{V}_2 also cancels in η .

To summarise, the explicit parametrisations of the Yukawa couplings Y_D in terms of η are

$$Y_D^{\text{polar}} = \frac{\sqrt{2}}{v} (\eta^*)^{\frac{1}{2}} \mathcal{V}_2 M_R^T, \quad (25)$$

$$Y_D^{\text{QR}} = \frac{1}{v} L \mathcal{V}_2 M_R^T \quad \text{with} \quad \eta = \frac{1}{2} L^* L^T, \quad (26)$$

$$Y_D^{\text{SVD}} = \frac{1}{v} \mathcal{V}_1 \text{diag}(y_1, y_2, y_3) \mathcal{V}_2 M_R^T \quad \text{with} \quad \eta = \frac{1}{2} \mathcal{V}_1^* \text{diag}(y_1^2, y_2^2, y_3^2) \mathcal{V}_1^T. \quad (27)$$

In all cases, we stress that due to the presence of M_R^T in the rightmost position in all the above expressions for Y_D , the connection to low-energy constraints (encoded in η) is valid for all possible invertible M_R . Thus, one directly parametrises the mixing between the active and sterile states rather than relying on “unphysical” Yukawa couplings. Moreover, the mixing amongst the heavy states is encoded in \mathcal{V}_2 .

In particular, it is worth highlighting that taking $\mathcal{V}_2 \neq \mathbb{1}$ to be non-trivial leads to an additional mixing in flavour-violation space, if the usual GIM-like suppression is broken by having non-degenerate heavy states. This can be understood as follows: the loop function entering the widths for radiative decays $\ell_\alpha \rightarrow \ell_\beta \gamma$ asymptotically tends to a constant for $M_R \gg m_W$ [38] as

$$G_\gamma(x) = -\frac{x(2x^2 + 5x - 1)}{4(1-x)^3} - \frac{3x^3}{2(1-x)^4} \log x, \quad (28)$$

$$G_\gamma(x) \xrightarrow{x \gg 1} \frac{1}{2}, \quad (29)$$

⁴Contrary to the other two parametrisations we have so far discussed, the parametrisation of Eq. (21), which relies on a singular value decomposition of Y_D , can likely be generalised to “asymmetric” versions of the Inverse Seesaw making use of the properties of left- and/or right-invertible rectangular m_D and M_R matrices. A dedicated study of this more general case lies outside the scope of the present work.

where $x = M_N^2/m_W^2$ and M_N is the mass of the heavy internal fermion. For Z -penguins (and for simplicity we take here the part which depends only on one internal fermion mass, and at vanishing momentum transfer), the loop functions asymptotically admit a logarithmic dependence on x as [38]

$$F_Z(x) = -\frac{5x}{2(1-x)} - \frac{5x^2}{2(1-x)^2} \log x, \quad (30)$$

$$F_Z(x) \xrightarrow{x \gg 1} \frac{5}{2} - \frac{5}{2} \log(x). \quad (31)$$

The dependence on mixing elements for a non-degenerate heavy spectrum is in general more complicated, and the impact of cLFV bounds on the off-diagonal elements of η is model-dependent, as discussed in [37]. Consequently, the different parametrisations outlined here will lead to different results for cLFV processes generated by anything other than just dipole operators, due to the different matrix structures that enter Y_D (see Eqs. (25-27)).

3 Future cLFV searches and EW precision measurements

As mentioned in previous sections, we will investigate in detail how different parametrisations of the ISS(3,3) allow to better control the contributions for an extensive set of observables, including those sensitive to the violation of lepton flavour universality, and those signalling lepton flavour violation. The role of these sets of observables has been widely explored in the framework of SM model extensions via heavy sterile states. For the case of cLFV leptonic transitions (as radiative decays, three-body decays and conversion in nuclei, among others), the corresponding form-factors and loop functions - common to generic variants of type I seesaw - can be found in [2, 14, 17, 20, 38–51]; for the ISS(3,3), cLFV Z -boson and Higgs decays have also been investigated [22, 32, 34]. Several Z -pole observables (including EW precision observables) have been recently evaluated at one-loop level, and a detailed discussion can be found in [23]. In Table 1 we summarise the current bounds and future sensitivities for several low- and high-energy cLFV observables.

A recent study of the prospects of an asymmetric $\mu^+ - e^-$ collider for the discovery of cLFV transitions (induced from the presence of heavy neutral leptons) has shown that a facility as μ TRISTAN can be particularly sensitive to flavour violation in $\tau - \ell$ transitions [52]. Here we will also consider the prospects of the ISS(3,3) for such a collider, setting a sensitivity threshold of 10 detected events (with a signal efficiency of 1%) for projected luminosities of 100 fb^{-1} and 1000 fb^{-1} .

Likewise, in Table 2, we present current experimental measurements and SM predictions for several LFUV and EW observables which will be subsequently discussed in the phenomenological analysis.

Concerning the projections for FCC-ee, in particular for Z -pole observables [74, 75], it is expected that uncertainties in $R_{\alpha\beta}(Z \rightarrow \ell\ell)$ will be reduced to 5×10^{-5} , the determination of $\Gamma(Z \rightarrow \ell\ell)$ be improved by a factor $\sim 50 - 500$, while for the T -parameter one expects⁵ $T \lesssim 0.0058$ [76].

Let us also notice that for other EW observables we will assume a mild improvement by a factor 10 of the associated uncertainties, and display the contours at 95% C.L. upon presentation of our results (solid lines will systematically denote a projection of future uncertainties under the assumption that the central value remains the current one, while dashed lines correspond to assuming that the central experimental value will evolve towards the SM prediction).

Although we will not offer a detailed discussion here, numerous low-energy processes are sensitive probes to NP sources of lepton flavour universality violation. This is the case of leptonic kaon and pion decays, τ -lepton decays, super-allowed beta decays, among many others. For simplicity, these constraints can be conveniently encoded in bounds on the diagonal entries of the η -matrix. Below we list the results of a recent analysis [37] (at 95% C.L.):

$$\begin{aligned} \eta_{ee} &\lesssim 1.4 \times 10^{-3}, \\ \eta_{\mu\mu} &\lesssim 1.4 \times 10^{-4}, \\ \eta_{\tau\tau} &\lesssim 8.9 \times 10^{-4}. \end{aligned} \quad (32)$$

⁵Here we take the most conservative estimate in which one assumes no further reduction of intrinsic theoretical uncertainties from missing higher order corrections, as well as no significant improvement of the parametric uncertainties.

Observable	Current bound	Future sensitivity
BR($\mu \rightarrow e\gamma$)	$< 3.1 \times 10^{-13}$ (MEG II [53])	6×10^{-14} (MEG II [54])
BR($\tau \rightarrow e\gamma$)	$< 3.3 \times 10^{-8}$ (BaBar [55])	3×10^{-9} (Belle II [56])
BR($\tau \rightarrow \mu\gamma$)	$< 4.2 \times 10^{-8}$ (Belle [57])	10^{-9} (Belle II [56])
BR($\mu \rightarrow 3e$)	$< 1.0 \times 10^{-12}$ (SINDRUM [58])	$10^{-15(-16)}$ (Mu3e [59])
BR($\tau \rightarrow 3e$)	$< 2.7 \times 10^{-8}$ (Belle [60])	5×10^{-10} (Belle II [56])
BR($\tau \rightarrow 3\mu$)	$< 1.9 \times 10^{-8}$ (Belle II [61])	5×10^{-10} (Belle II [56]) 5×10^{-11} (FCC-ee [62])
CR($\mu - e, N$)	$< 7 \times 10^{-13}$ (Au, SINDRUM [63])	10^{-14} (SiC, DeeMe [64]) 2.6×10^{-17} (Al, COMET [65–67]) 8×10^{-17} (Al, Mu2e [68])
BR($Z \rightarrow e^\pm \mu^\mp$)	$< 4.2 \times 10^{-7}$ (ATLAS [69])	$\mathcal{O}(10^{-10})$ (FCC-ee [62])
BR($Z \rightarrow e^\pm \tau^\mp$)	$< 4.1 \times 10^{-6}$ (ATLAS [70])	$\mathcal{O}(10^{-10})$ (FCC-ee [62])
BR($Z \rightarrow \mu^\pm \tau^\mp$)	$< 5.3 \times 10^{-6}$ (ATLAS [70])	$\mathcal{O}(10^{-10})$ (FCC-ee [62])

Table 1: Current experimental bounds and future sensitivities on relevant cLFV observables. The quoted limits are given at 90% C.L. (Belle II sensitivities correspond to an integrated luminosity of 50 ab^{-1} .)

Observable	Exp. Measurement	SM prediction
$R_{\mu e}(Z \rightarrow \ell\ell)$	1.0001 ± 0.0024 (PDG [71])	1.0 [72]
$R_{\tau e}(Z \rightarrow \ell\ell)$	1.0020 ± 0.0032 (PDG [71])	0.9977 [72]
$R_{\tau\mu}(Z \rightarrow \ell\ell)$	1.0010 ± 0.0026 (PDG [71])	0.9977 [72]
$\Gamma(Z \rightarrow e^+e^-)$	$83.91 \pm 0.12 \text{ MeV}$ (LEP [73])	$83.965 \pm 0.016 \text{ MeV}$ [72]
$\Gamma(Z \rightarrow \mu^+\mu^-)$	$83.99 \pm 0.18 \text{ MeV}$ (LEP [73])	$83.965 \pm 0.016 \text{ MeV}$ [72]
$\Gamma(Z \rightarrow \tau^+\tau^-)$	$84.08 \pm 0.22 \text{ MeV}$ (LEP [73])	$83.775 \pm 0.016 \text{ MeV}$ [72]
$\Gamma(Z \rightarrow \text{inv.})$	$499.0 \pm 1.5 \text{ MeV}$ (PDG [71])	$501.45 \pm 0.05 \text{ MeV}$ [72]

Table 2: Experimental measurements and SM predictions for several LFUV and EW observables discussed in the phenomenological analysis. All uncertainties are given at 68% C.L., while for the SM predictions of the universality ratios, the parametric uncertainties are negligible.

4 Results: exploring the ISS(3,3) parameter space

After the formal discussion of the different techniques to parametrise the new sources of flavour violation that emerge within the Inverse Seesaw, we now proceed to illustrate their comparative potential. Starting from the most simple possibility of a modified Casas-Ibarra parametrisation, we then proceed to consider more sophisticated means of encoding flavour violation, be it between active-sterile states, or in direct connection to the heavy sterile sector. We will further discuss how the “entanglement” of sources of flavour violation can be systematically analysed via the parametrisations developed in Section 2. Throughout this section we assume the light spectrum to be “normal ordered”, and fix oscillation data to the current central values [77], further setting the lightest neutrino mass to 10^{-5} eV .

4.1 Simplified scenarios

We begin our discussion by a simple - yet illustrative - case, relying in the ISS-modified Casas-Ibarra parametrisation (cf. Eq. (4)). Taking M_R and μ_X as diagonal and universal, and setting $R = \mathbb{1}$, we display in Figure 1 several leptonic cLFV processes, separately focusing on $\mu - e$ and $\tau - \ell$ transitions. Shaded regions denote constraints from current experimental bounds on various cLFV processes, while

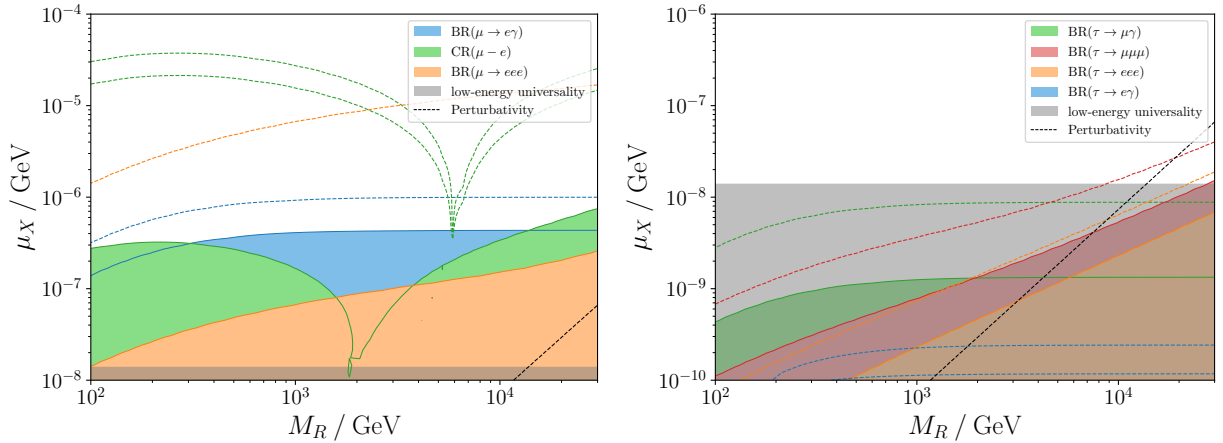


Figure 1: Casas-Ibarra parametrisation: constraints on the ISS(3,3) parameter space from current bounds and future sensitivities on several cLFV observables, in the $\mu - e$ (left panel) and $\tau - \ell$ (right panel) sectors, together with the bound from fits to low-energy lepton universality observables from [37]. We have set $R = \mathbb{1}$ and assume M_R and μ_X to be degenerate. Current bounds correspond to shaded regions while future sensitivities are indicated by dashed lines (see Table 1 for further details). Dark grey regions correspond to exclusion from low-energy universality bounds, while dashed black lines reflect non-perturbative Yukawa couplings.

dashed lines denote the future sensitivity of upcoming (or already running) cLFV experiments. Note that for neutrinoless $\mu - e$ conversion we display the two most sensitive projections of the COMET and Mu2e experiments (see Table 1). We further display the current upper bound on $\text{Tr}(\eta)$ obtained in [37] and highlight regimes associated with non-perturbative Yukawa couplings, i.e. $Y_D^{ij} \geq \sqrt{4\pi}$.

As can be seen in the two plots in Figure 1, the contributions for $\mu - e$ flavour violating and τ -lepton related observables are strongly entangled with each other and cannot be separately analysed. This is a consequence of having a unique “source” of flavour violation - the (non-unitary) PMNS matrix. In order to evade the stringent constraints from data on low-energy universality observables (which do exclude important regions of the $\mu_X - M_R$ parameter space) as well as bounds on $\mu - e$ flavour violating transitions, one could in principle finely tune the complex angles in the R -matrix appearing in Eq. (4), but there is no clear indication on the path to take. One could further assume a non-minimal flavour structure in μ_X and/or M_R , but also this approach does not offer a simple connection to η due to the non-linear appearance of μ_X and M_R in Eq. (4).

Instead of relying on the Casas-Ibarra parametrisation, we take the proposed parametrisation shown in Eq. (21), using a numerical eigenvalue decomposition of η to fix Y_D entirely from low-energy universality data (encoded in η_{ii}) up to \mathcal{V}_2 , which we take as trivial, i.e. $\mathcal{V}_2 = \mathbb{1}$. In this way, we only parametrise the mixing between active and sterile states while neglecting potential mixings exclusive to the sterile states. At this stage, we will assume the heavy spectrum to be degenerate: in other words, we take M_R to be diagonal and universal.

To begin with, let us then analyse the impact of the mixing of a single heavy pseudo-Dirac pair with the active sector, which can be parametrised via one of the diagonal η_{ii} . In this limit (one heavy pair mixing with one active flavour, and degenerate heavy states) cLFV can only be mediated by light neutrino exchange and is therefore negligible. In Figure 2 we show exclusion contours of current experimental data and future sensitivities of several Z -pole observables in the plane spanned by a single η_{ii} and the mass of the (degenerate) heavy spectrum M_R . Notice that the contour from the low-energy fit [37], cf. Eq. (32), is independent of the heavy mass scale, since only tree-level LFUV observables have been taken into account⁶. The filled contours denote constraints from current data (see Table 2), and we also present two distinct projections for future FCC-ee data. Concerning the

⁶The authors of [37] in principle also take into account loop-level observables via (tree-level) modifications of the Fermi constant G_F , which feed back into electroweak loops that appear, for instance, in corrections to M_W . The presence of BSM states in those loops is however neglected, such that the bounds on η are independent of the heavy mass scale.

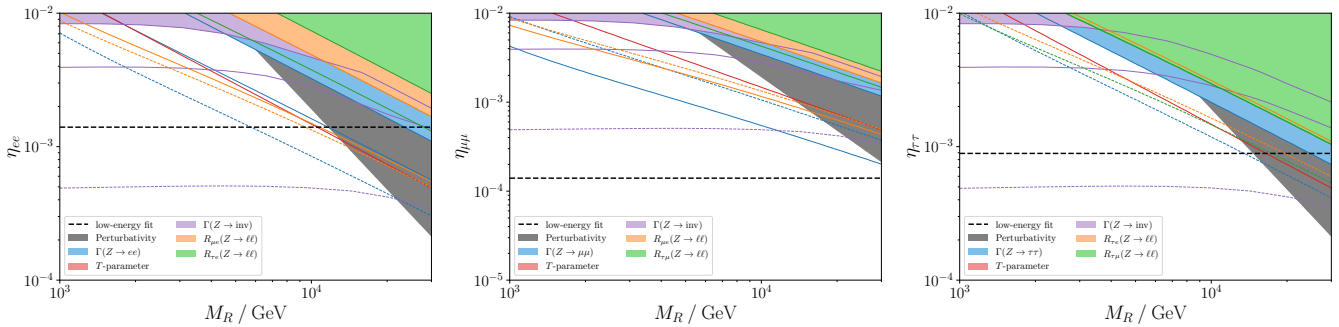


Figure 2: Constraints from current experimental bounds and future sensitivities from Z -pole observables, together with the bound of the low-energy fit on η_{ii} of [37]. From left to right, we consider one η_{ii} at a time (the others set to a negligible value) and vary the mass of the heavy states M_R (assumed degenerate). All contours are shown at 95% C.L..

latter, and as discussed in the previous section, we assume a rather mild improvement of only one order of magnitude of the uncertainties of Z -pole observables due to the unprecedented luminosity of a Tera- Z run at a future e^+e^- machine. For the central value of the future measurement, we assume current data (solid lines) or the SM expectation (dashed lines). In the right-most plot of Figure 2, due to a minor tension between the measurement of $Z \rightarrow \tau\tau$ and its SM prediction, the entire plane would be excluded should the central value of $\Gamma(Z \rightarrow \tau\tau)$ remain the same. (The predictions for all observables shown in Figure 2 have been computed relying on the results derived in [23].) In all plots of Fig. 2 it can be seen that the NLO corrections to the Z -pole observables induced by the presence of heavy sterile states might become important in the future, but as far as LEP data is concerned they can safely be neglected. A more dedicated analysis, also including W and Higgs observables (concerning a potential violation of lepton flavour universality) can be found in [23].

We continue by carrying out a complementary approach, focusing on the behaviour of flavour violating observables with respect to the off-diagonal entries of η . As outlined in Section 3, we consider several cLFV observables at low-energies, at the Z -pole, as well as at a possible future μ TRISTAN collider, as recently explored in [52].

For heavy and degenerate masses M_R , the branching ratios of the cLFV radiative decays are well approximated by

$$\text{BR}(\ell_\alpha \rightarrow \ell_\beta \gamma) \simeq \frac{3\alpha}{2\pi} |\eta_{\alpha\beta}|^2, \quad (33)$$

due to the aforementioned behaviour of the loop-function entering in the amplitude of the decay (see Eqs. (28, 29)). This is not the case for the Z -penguins appearing in $\mu \rightarrow 3e$ and neutrinoless $\mu - e$ conversion in muonic atoms, which retain a logarithmic dependence on the heavy mass scale, as illustrated in Eq. (31).

In what follows, we now fix the diagonal entries of η to their maximum values as shown in Eq. (32) and vary the degenerate heavy mass scale and one off-diagonal η_{ij} at a time (up to its maximum as allowed by the Schwarz inequality, see Eq. (15)), while the others, as well as all phases, have been set to 0. As shown in the left-most plot of Figure 3, the constraints on $\eta_{e\mu}$ derived from either current bounds or future sensitivities (respectively filled contours and dashed lines) on $\mu \rightarrow e\gamma$ are nearly independent of M_R , while constraints from other observables (which are mediated by Z -penguins and box topologies) grow stronger for increasing M_R , as expected. We also recover the “dip” in $\mu - e$ conversion, which is due to a destructive interference between different contributing topologies, and whose position depends on the considered nucleus. Notice that the current bound for $\mu - e$ conversion was obtained using Gold as a target material, while the two sensitivity projections for the COMET and Mu2e experiments (see Table 1) rely on Aluminium, thus shifting the “dip” to a different position.

In the remaining plots of Figure 3 the focus lies on the $\tau - \ell$ sectors. We display the constraints from future sensitivities of $\tau \rightarrow 3\ell$, $Z \rightarrow \tau^\pm \ell^\mp$, as well as the projected sensitivities of the preliminary μ TRISTAN analysis of [52]. As already shown in [52], future constraints that can be obtained at μ TRISTAN on $\eta_{e\tau}$ and $\eta_{\mu\tau}$ from cLFV processes mediated via $\tau - e$ and $\tau - \mu$ Z -penguins will

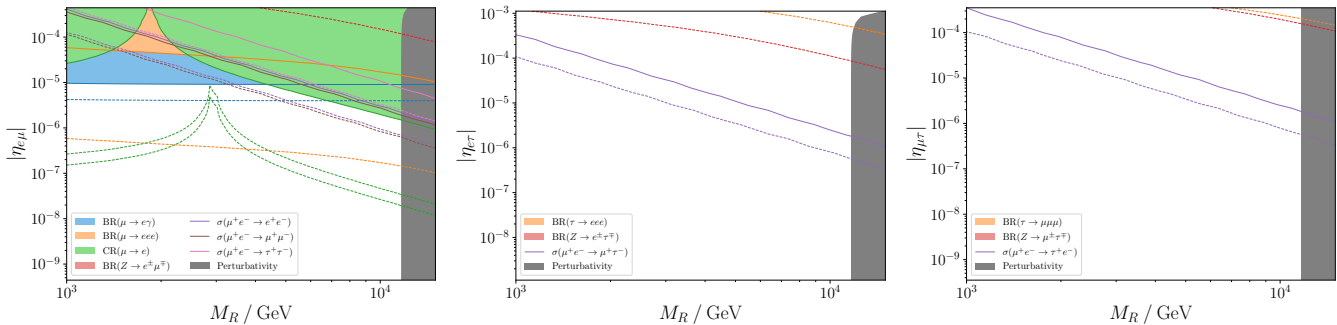


Figure 3: Constraints from current experimental bounds (filled contours) and future sensitivities (dashed lines) from low-energy and Z -pole cLFV observables, together with the projected reach of the μ TRISTAN collider from [52], assuming luminosities of 100fb^{-1} (solid lines) and 1ab^{-1} (dashed lines). From left to right, we take one off-diagonal η_{ij} at a time (with the others set to zero), varying the mass of the heavy states M_R (assumed degenerate). The diagonal η_{ii} have been set to their maximally allowed values as obtained in [37].

strongly outperform bounds stemming both from low-energy cLFV processes and Z -pole searches at a future Tera- Z factory (even with the most optimistic assumptions about systematic uncertainties); in contrast future $\mu - e$ dedicated facilities will always yield the strongest bounds on $\eta_{e\mu}$.

4.2 Impact of non-degenerate heavy spectra

As argued in the previous subsection, the off-diagonal entries η_{ij} have a direct connection with radiative decays $\ell_\alpha \rightarrow \ell_\beta \gamma$ (which are asymptotically independent of the heavy mass scale), in contrast to other cLFV transitions which are dominated by Z -penguin exchange. Moreover, it is important to emphasise that if the heavy spectrum is non-degenerate, the Z -penguin mediated processes also depend on a potentially non-trivial flavour structure of the heavy spectrum itself. In turn, this implies that one can no longer ignore the role of \mathcal{V}_2 in the parametrisations derived in Section 2, and it is expected that it will have an impact on the observables. Throughout the remainder of this section, and to illustrate the impact of a non-degenerate heavy spectrum, we consider a benchmark hierarchy, setting $M_R = \text{diag}(0.9, 1, 1.1) M_0$. Since we aim at isolating the role of a non-trivial $\mathcal{V}_2 \neq \mathbb{1}$, we thus set the off-diagonal $\eta_{ij} = 0$, while keeping the diagonal η_{ii} at their maximal values as before (see Eq. (32)). To start with, we vary the overall heavy mass scale M_0 , and consider the effect of one angle $\sin \theta_{ij} \neq 0$ of \mathcal{V}_2 (with the others set to 0), see Eq. (22).

In Figure 4 we present the exclusion contours from current data on cLFV (coloured surfaces) as well as the projected reach of dedicated cLFV facilities and that of cLFV searches at μ TRISTAN (dashed lines). Even if the off-diagonal entries of η have been set to 0, processes such as $\mu \rightarrow 3e$ and neutrinoless $\mu - e$ conversion in muonic atoms - which receive dominant penguin contributions in the ISS(3,3) - significantly constrain the angle $\sin \theta_{12}$ over a wide range of masses M_R . In this case, μ TRISTAN scattering observables only play a minor role. (The rate of the radiative decay $\mu \rightarrow e\gamma$ is negligible by construction.) In the remaining plots of Figure 4 we recover the leading role of μ TRISTAN for $\tau - \ell$ flavour-violating observables: the strongest (would-be) constraints on $\sin \theta_{13}$ and $\sin \theta_{23}$ would be obtained by μ TRISTAN, while other penguin transitions contributing to low-energy observables and Z -pole cLFV are predicted to have very small rates.

To further demonstrate the impact of mixing amongst the heavy states, we now consider the effect of simultaneously varying two mixing angles of \mathcal{V}_2 (the remaining one set to 0). The masses of the three heavy pseudo-Dirac pairs are fixed to $M_R = \text{diag}(9, 10, 11) \text{TeV}$. The results of this analysis are shown in Figure 5, with the same colour code as above. In the left plot we vary $\sin \theta_{12}$ and $\sin \theta_{13}$. As can be seen, there is a manifest interplay between the two mixings; having a large $\sin \theta_{13}$ leads to the suppression of the $\mu - e$ cLFV rates - induced by $\sin \theta_{12}$ - and vice versa. Remarkably, the simultaneous presence of both further induces cLFV rates in the $\mu - \tau$ “direction”: one can phenomenologically interpret this as a leakage of flavour-violation from the $\mu - e$ and $\tau - e$ directions to the $\mu - \tau$ one.

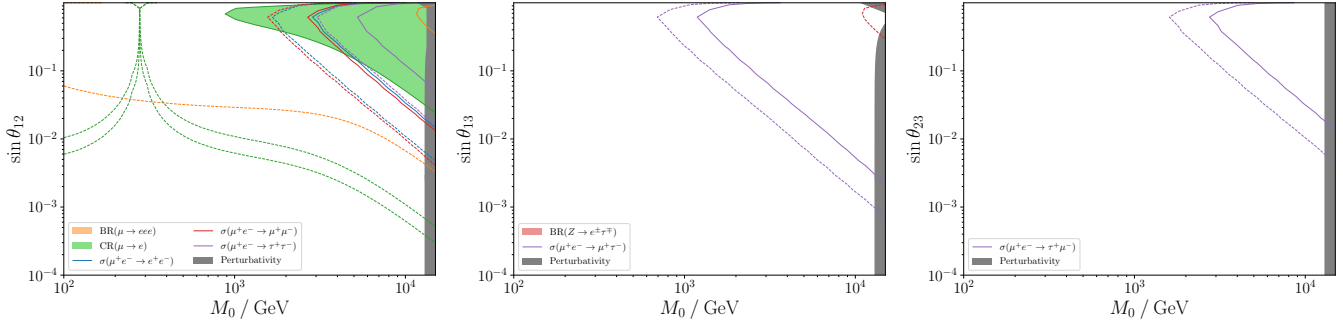


Figure 4: Constraints from current experimental bounds (filled contours) and future sensitivities (dashed lines) from low-energy and Z -pole cLFV observables, together with the projected cLFV reach of a μ TRISTAN collider from [52], assuming luminosities of 100 fb^{-1} (solid lines) and 1 ab^{-1} (dashed lines). From left to right, we vary one of the angles of \mathcal{V}_2 (see Eq. (21)) at a time with the other angles set to zero, versus the mass scale of the heavy states M_0 (assuming a non-degenerate spectrum with $M_R = \text{diag}(0.9, 1, 1.1) M_0$). The off-diagonal η_{ij} have been also set to zero, and the diagonal η_{ii} to their maximally allowed values as obtained in [37].

This becomes all the more striking in the right plot of Figure 5, where we vary $\sin \theta_{13}$ and $\sin \theta_{23}$. Here, the simultaneous presence of both angles leads to sizeable rates for $\mu \rightarrow 3e$ as well as $\mu - e$ conversion, albeit still in a sub-leading way with respect to the potential μ TRISTAN sensitivities.

Finally, one can also consider the simultaneous presence of off-diagonal η_{ij} and of non-vanishing mixing angles $\sin \theta_{ij}$ in \mathcal{V}_2 . This leads to more complicated mixing regimes in which it becomes challenging to disentangle the sources of flavour violation: between active and sterile states, or mixing among the heavy sterile states. The only exception to this is, as discussed, γ -penguin contributions.

As previously argued, the γ dipoles are to a very good approximation only proportional to one of the off-diagonal η_{ij} . Consequently, contributions from γ -dipoles can be “switched off” by construction – and thus it is possible to have sizeable rates for $\mu \rightarrow 3e$ and neutrinoless $\mu - e$ conversion in muonic atoms (induced by sizeable η_{ii} and non-trivial mixing in the heavy sector) while having negligible rates for $\mu \rightarrow e\gamma$. The observation of such a pattern for the cLFV observables could ultimately hint at a non-degenerate and non-trivially mixed heavy spectrum.

5 Concluding remarks

In this work we have considered an inverse seesaw mechanism with $3 + 3$ heavy sterile states. Based on simple algebraic arguments, we developed new parametrisations of the Yukawa couplings that allow directly incorporating flavour misalignment stemming from the deviation from unitarity of the 3×3 would-be PMNS block of the full unitary lepton mixing matrix. This deviation is conveniently encoded in the “ η -matrix”, which can be constrained by fits to low-energy data in a model independent way. Consequently, and by construction, the new parametrisations we proposed here allow for a “safe” exploration of the ISS(3,3) viable parameter space, and one can systematically access different directions in “flavour-violation space”. We have then further studied this direct connection to low-energy data in a dedicated phenomenological analysis of numerous cLFV and lepton universality observables at low energies, at the Z -pole (at past and future lepton colliders), as well as at a possible μ^+e^- μ TRISTAN collider.

While $\mu \rightarrow e$ dedicated facilities will be able to set the strongest bounds on mixings associated with the first two generations, cLFV searches at μ TRISTAN would improve the sensitivity to flavour violation in the $e\tau$ and $\mu\tau$ sectors by several orders of magnitude with respect to dedicated searches at the Z -pole. Our results reveal interesting synergies of the different cLFV observables and their constraining power to disentangle different sources of flavour violation: in particular, and as we have argued, they might allow distinguishing the flavour mixing between active and sterile neutrinos from mixing exclusively occurring amongst the heavy states.

We ultimately point out that in the absence of a signal in the $\mu \rightarrow e\gamma$ channel, future measurements

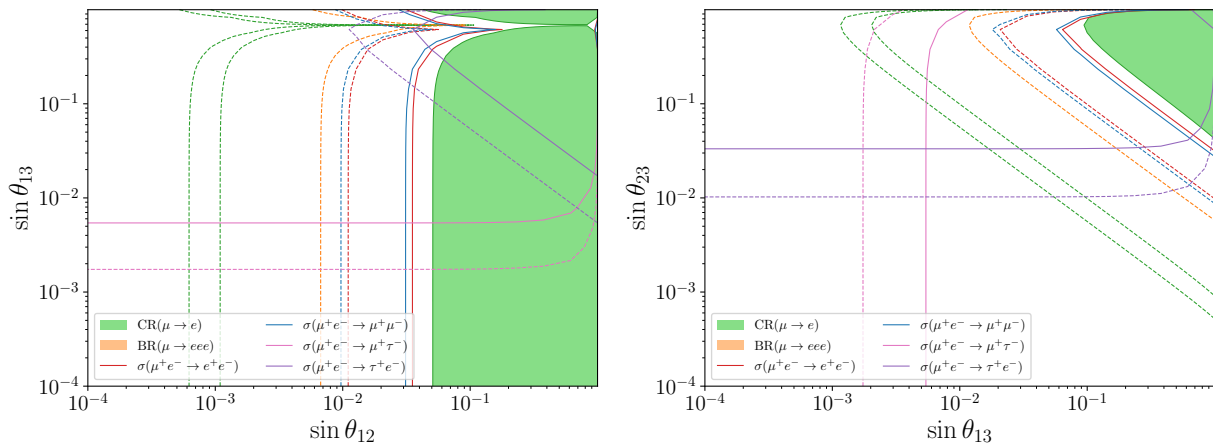


Figure 5: Constraints from current experimental bounds (filled contours) and future sensitivities (dashed lines) from low-energy and Z -pole cLFV observables, together with the projected reach of a μ TRISTAN collider from [52], assuming luminosities of 100 fb^{-1} (solid lines) and 1 ab^{-1} (dashed lines). On each panel we vary two of the angles of \mathcal{V}_2 (see Eq. (21)) at a time with the other, as well as the off-diagonal η_{ij} , set to zero. The heavy spectrum has been fixed to $M_R = \text{diag}(9, 10, 11) \text{ TeV}$. The diagonal η_{ii} have been set to their maximally allowed values as obtained in [37].

of sizeable rates for $\mu \rightarrow 3e$ and neutrinoless $\mu-e$ conversion in muonic atoms could hint at the presence of a non-trivially mixed and non-degenerate heavy spectrum.

Although all parametrisations are formally equivalent (and do lead to the same physical results), here our goal was to develop a systematic access to phenomenological interesting regimes, exhibiting different flavour (and non-universality) features. Moreover, the analytical results of this work lead to a direct and simple connection to low-energy data, which allows for a “safe” implementation in Feynrules [78, 79]. This opens the door for phenomenological collider studies, which can be carried out while easily avoiding stringent constraints from low-energy cLFV and LFUV bounds.

Acknowledgements

We are grateful to Emanuelle Pinsard for a careful reading of the manuscript. JK is supported by the Slovenian Research Agency under the research grant No. N1-0253 and in part by J1-3013. This project has received support from the European Union’s Horizon 2020 research and innovation programme under the Marie Skłodowska-Curie grant agreement No. 860881 (HIDDe ν network) and from the IN2P3 (CNRS) Master Project, “Hunting for Heavy Neutral Leptons” (12-PH-0100).

A Cholesky decomposition of η

Applying the Cholesky-Banachiewicz algorithm on a $n \times n$ matrix of small order n can be easily done by hand. In the case of a complex hermitian 3×3 matrix A the Cholesky-decomposition $A = LL^\dagger$ is thus found as

$$\begin{aligned}
 L_{i,i} &= \sqrt{A_{i,i} - \sum_{k=1}^{i-1} |L_{i,k}|^2}, \\
 L_{i,j} &= \frac{1}{L_{j,j}} \left(A_{i,j} - \sum_{k=1}^{j-1} L_{i,k} L_{j,k}^* \right) \quad \text{for } i > j.
 \end{aligned} \tag{34}$$

Furthermore, the inverse of the lower triangular matrix L is easily found as

$$L^{-1} = \begin{pmatrix} \frac{1}{L_{1,1}} & 0 & 0 \\ -\frac{L_{2,1}}{L_{1,1} L_{2,2}} & \frac{1}{L_{2,2}} & 0 \\ -\frac{L_{2,2} L_{3,1} - L_{2,1} L_{3,2}}{L_{1,1} L_{2,2} L_{3,3}} & -\frac{L_{3,2}}{L_{2,2} L_{3,3}} & \frac{1}{L_{3,3}} \end{pmatrix}. \quad (35)$$

References

- [1] J. Schechter and J.W.F. Valle, *Neutrino Masses in $SU(2) \times U(1)$ Theories*, *Phys. Rev. D* **22** (1980) 2227.
- [2] M. Gronau, C.N. Leung and J.L. Rosner, *Extending Limits on Neutral Heavy Leptons*, *Phys. Rev. D* **29** (1984) 2539.
- [3] R.N. Mohapatra and J.W.F. Valle, *Neutrino Mass and Baryon Number Nonconservation in Superstring Models*, *Phys. Rev. D* **34** (1986) 1642.
- [4] P. Minkowski, *$\mu \rightarrow e\gamma$ at a Rate of One Out of 10^9 Muon Decays?*, *Phys. Lett. B* **67** (1977) 421.
- [5] T. Yanagida, *Horizontal gauge symmetry and masses of neutrinos*, *Conf. Proc. C* **7902131** (1979) 95.
- [6] S.L. Glashow, *The Future of Elementary Particle Physics*, *NATO Sci. Ser. B* **61** (1980) 687.
- [7] M. Gell-Mann, P. Ramond and R. Slansky, *Complex Spinors and Unified Theories*, *Conf. Proc. C* **790927** (1979) 315 [1306.4669].
- [8] R.N. Mohapatra and G. Senjanovic, *Neutrino Mass and Spontaneous Parity Nonconservation*, *Phys. Rev. Lett.* **44** (1980) 912.
- [9] G. 't Hooft, C. Itzykson, A. Jaffe, H. Lehmann, P.K. Mitter, I.M. Singer et al., eds., *Recent Developments in Gauge Theories. Proceedings, Nato Advanced Study Institute, Cargese, France, August 26 - September 8, 1979*, vol. 59, 1980. 10.1007/978-1-4684-7571-5.
- [10] H. Hettmansperger, M. Lindner and W. Rodejohann, *Phenomenological Consequences of sub-leading Terms in See-Saw Formulas*, *JHEP* **04** (2011) 123 [1102.3432].
- [11] P.S.B. Dev and A. Pilaftsis, *Minimal Radiative Neutrino Mass Mechanism for Inverse Seesaw Models*, *Phys. Rev. D* **86** (2012) 113001 [1209.4051].
- [12] A. Abada and M. Lucente, *Looking for the minimal inverse seesaw realisation*, *Nucl. Phys. B* **885** (2014) 651 [1401.1507].
- [13] A. Abada, V. De Romeri and A.M. Teixeira, *Effect of sterile states on lepton magnetic moments and neutrinoless double beta decay*, *JHEP* **09** (2014) 074 [1406.6978].
- [14] A. Abada, M.E. Krauss, W. Porod, F. Staub, A. Vicente and C. Weiland, *Lepton flavor violation in low-scale seesaw models: SUSY and non-SUSY contributions*, *JHEP* **11** (2014) 048 [1408.0138].
- [15] A. Abada, V. De Romeri, S. Monteil, J. Orloff and A.M. Teixeira, *Indirect searches for sterile neutrinos at a high-luminosity Z-factory*, *JHEP* **04** (2015) 051 [1412.6322].
- [16] E. Arganda, M.J. Herrero, X. Marcano and C. Weiland, *Enhancement of the lepton flavor violating Higgs boson decay rates from SUSY loops in the inverse seesaw model*, *Phys. Rev. D* **93** (2016) 055010 [1508.04623].
- [17] A. Abada, V. De Romeri and A.M. Teixeira, *Impact of sterile neutrinos on nuclear-assisted cLFV processes*, *JHEP* **02** (2016) 083 [1510.06657].
- [18] A. Abada, A. Hernández-Cabezudo and X. Marcano, *Beta and Neutrinoless Double Beta Decays with KeV Sterile Fermions*, *JHEP* **01** (2019) 041 [1807.01331].
- [19] A. Abada and T. Toma, *Electric dipole moments of charged leptons in models with pseudo-Dirac sterile fermions*, *JHEP* **08** (2024) 128 [2405.01648].
- [20] E. Arganda, M.J. Herrero, X. Marcano and C. Weiland, *Imprints of massive inverse seesaw model neutrinos in lepton flavor violating Higgs boson decays*, *Phys. Rev. D* **91** (2015) 015001 [1405.4300].
- [21] V. De Romeri, M.J. Herrero, X. Marcano and F. Scarcella, *Lepton flavor violating Z decays: A promising window to low scale seesaw neutrinos*, *Phys. Rev. D* **95** (2017) 075028 [1607.05257].
- [22] A. Abada, J. Kriewald, E. Pinsard, S. Rosauro-Alcaraz and A.M. Teixeira, *LFV Higgs and Z-boson decays: leptonic CPV phases and CP asymmetries*, *Eur. Phys. J. C* **83** (2023) 494 [2207.10109].

- [23] A. Abada, J. Kriewald, E. Pinsard, S. Rosauero-Alcaraz and A.M. Teixeira, *Heavy neutral lepton corrections to SM boson decays: lepton flavour universality violation in low-scale seesaw realisations*, *Eur. Phys. J. C* **84** (2024) 149 [2307.02558].
- [24] Y. Cai, T. Han, T. Li and R. Ruiz, *Lepton Number Violation: Seesaw Models and Their Collider Tests*, *Front. in Phys.* **6** (2018) 40 [1711.02180].
- [25] S. Pascoli, R. Ruiz and C. Weiland, *Heavy neutrinos with dynamic jet vetoes: multilepton searches at $\sqrt{s} = 14, 27, \text{ and } 100 \text{ TeV}$* , *JHEP* **06** (2019) 049 [1812.08750].
- [26] A. Abada, P. Escribano, X. Marcano and G. Piazza, *Collider searches for heavy neutral leptons: beyond simplified scenarios*, *Eur. Phys. J. C* **82** (2022) 1030 [2208.13882].
- [27] J.A. Casas and A. Ibarra, *Oscillating neutrinos and $\mu \rightarrow e, \gamma$* , *Nucl. Phys. B* **618** (2001) 171 [hep-ph/0103065].
- [28] J.A. Casas, J.M. Moreno, N. Rius, R. Ruiz de Austri and B. Zaldivar, *Fair scans of the seesaw. Consequences for predictions on LFV processes*, *JHEP* **03** (2011) 034 [1010.5751].
- [29] E. Fernandez-Martinez, M.B. Gavela, J. Lopez-Pavon and O. Yasuda, *CP-violation from non-unitary leptonic mixing*, *Phys. Lett. B* **649** (2007) 427 [hep-ph/0703098].
- [30] A. Broncano, M.B. Gavela and E.E. Jenkins, *The Effective Lagrangian for the seesaw model of neutrino mass and leptogenesis*, *Phys. Lett. B* **552** (2003) 177 [hep-ph/0210271].
- [31] D. Zhang and S. Zhou, *Complete one-loop matching of the type-I seesaw model onto the Standard Model effective field theory*, *JHEP* **09** (2021) 163 [2107.12133].
- [32] E. Arganda, M.J. Herrero, X. Marcano and C. Weiland, *Imprints of massive inverse seesaw model neutrinos in lepton flavor violating Higgs boson decays*, *Phys. Rev. D* **91** (2015) 015001 [1405.4300].
- [33] J.C. Garnica, G. Hernández-Tomé and E. Peinado, *Charged lepton-flavor violating processes and suppression of nonunitary mixing effects in low-scale seesaw models*, *Phys. Rev. D* **108** (2023) 035033 [2302.07379].
- [34] V. De Romeri, M.J. Herrero, X. Marcano and F. Scarcella, *Lepton flavor violating Z decays: A promising window to low scale seesaw neutrinos*, *Phys. Rev. D* **95** (2017) 075028 [1607.05257].
- [35] J. Kriewald, M. Nemevšek and F. Nesti, *Enabling Precise Predictions for Left-Right Symmetry at Colliders*, 2403.07756.
- [36] E. Fernandez-Martinez, J. Hernandez-Garcia and J. Lopez-Pavon, *Global constraints on heavy neutrino mixing*, *JHEP* **08** (2016) 033 [1605.08774].
- [37] M. Blennow, E. Fernández-Martínez, J. Hernández-García, J. López-Pavón, X. Marcano and D. Naredo-Tuero, *Bounds on lepton non-unitarity and heavy neutrino mixing*, *JHEP* **08** (2023) 030 [2306.01040].
- [38] A. Ilakovac and A. Pilaftsis, *Flavor violating charged lepton decays in seesaw-type models*, *Nucl. Phys. B* **437** (1995) 491 [hep-ph/9403398].
- [39] R. Alonso, M. Dhen, M.B. Gavela and T. Hambye, *Muon conversion to electron in nuclei in type-I seesaw models*, *JHEP* **01** (2013) 118 [1209.2679].
- [40] A. Abada and A.M. Teixeira, *Heavy neutral leptons and high-intensity observables*, *Front. in Phys.* **6** (2018) 142 [1812.08062].
- [41] A. Abada, J. Kriewald, E. Pinsard, S. Rosauero-Alcaraz and A.M. Teixeira, *LFV Higgs and Z-boson decays: leptonic CPV phases and CP asymmetries*, *Eur. Phys. J. C* **83** (2023) 494 [2207.10109].
- [42] T. Riemann and G. Mann, *NONDIAGONAL Z DECAY: $Z \rightarrow e \mu$* , in *10th International Conference on Neutrino Physics: Neutrino '82*, pp. 58–61, 1982.
- [43] J.I. Illana, M. Jack and T. Riemann, *Predictions for $Z \rightarrow \mu \tau$ and related reactions*, in *2nd Workshop of the 2nd Joint ECFA / DESY Study on Physics and Detectors for a Linear Electron Positron Collider*, pp. 490–524, 12, 1999 [hep-ph/0001273].
- [44] G. Mann and T. Riemann, *EFFECTIVE FLAVOR CHANGING WEAK NEUTRAL CURRENT IN THE STANDARD THEORY AND Z BOSON DECAY*, *Annalen Phys.* **40** (1984) 334.
- [45] J.I. Illana and T. Riemann, *Charged lepton flavor violation from massive neutrinos in Z decays*, *Phys. Rev. D* **63** (2001) 053004 [hep-ph/0010193].

- [46] E. Ma and A. Pramudita, *Flavor Changing Effective Neutral Current Couplings in the Weinberg-Salam Model*, *Phys. Rev. D* **22** (1980) 214.
- [47] F. Deppisch and J.W.F. Valle, *Enhanced lepton flavor violation in the supersymmetric inverse seesaw model*, *Phys. Rev. D* **72** (2005) 036001 [hep-ph/0406040].
- [48] F. Deppisch, T.S. Kosmas and J.W.F. Valle, *Enhanced $\mu - e$ conversion in nuclei in the inverse seesaw model*, *Nucl. Phys. B* **752** (2006) 80 [hep-ph/0512360].
- [49] D.N. Dinh, A. Ibarra, E. Molinaro and S.T. Petcov, *The $\mu - e$ Conversion in Nuclei, $\mu \rightarrow e\gamma$, $\mu \rightarrow 3e$ Decays and TeV Scale See-Saw Scenarios of Neutrino Mass Generation*, *JHEP* **08** (2012) 125 [1205.4671].
- [50] A. Abada, D. Bečirević, M. Lucente and O. Sumensari, *Lepton flavor violating decays of vector quarkonia and of the Z boson*, *Phys. Rev. D* **91** (2015) 113013 [1503.04159].
- [51] A. Abada, V. De Romeri, J. Orloff and A.M. Teixeira, *In-flight cLFV conversion: $e - \mu$, $e - \tau$ and $\mu - \tau$ in minimal extensions of the standard model with sterile fermions*, *Eur. Phys. J. C* **77** (2017) 304 [1612.05548].
- [52] J. Kriewald, E. Pinsard and A.M. Teixeira, *High-energy cLFV at μ TRISTAN: HNL extensions of the Standard Model*, 2412.04331.
- [53] MEG II collaboration, *A search for $\mu^+ \rightarrow e^+\gamma$ with the first dataset of the MEG II experiment*, *Eur. Phys. J. C* **84** (2024) 216 [2310.12614].
- [54] MEG II collaboration, *The design of the MEG II experiment*, *Eur. Phys. J. C* **78** (2018) 380 [1801.04688].
- [55] BABAR collaboration, *Searches for Lepton Flavor Violation in the Decays $\tau_{+-} \rightarrow e_{+-} \gamma$ and $\tau_{+-} \rightarrow \mu_{+-} \gamma$* , *Phys. Rev. Lett.* **104** (2010) 021802 [0908.2381].
- [56] BELLE-II collaboration, *The Belle II Physics Book*, *PTEP* **2019** (2019) 123C01 [1808.10567].
- [57] BELLE collaboration, *Search for lepton-flavor-violating tau-lepton decays to $\ell\gamma$ at Belle*, *JHEP* **10** (2021) 19 [2103.12994].
- [58] SINDRUM collaboration, *Search for the Decay $\mu^+ \rightarrow e^+e^+e^-$* , *Nucl. Phys. B* **299** (1988) 1.
- [59] A. Blondel et al., *Research Proposal for an Experiment to Search for the Decay $\mu \rightarrow eee$* , 1301.6113.
- [60] K. Hayasaka et al., *Search for Lepton Flavor Violating Tau Decays into Three Leptons with 719 Million Produced $\tau_{+}\tau_{-}$ Pairs*, *Phys. Lett. B* **687** (2010) 139 [1001.3221].
- [61] BELLE-II collaboration, *Search for lepton-flavor-violating $\tau^- \rightarrow \mu^- \mu^+ \mu^-$ decays at Belle II*, *JHEP* **09** (2024) 062 [2405.07386].
- [62] FCC collaboration, *FCC Physics Opportunities: Future Circular Collider Conceptual Design Report Volume 1*, *Eur. Phys. J. C* **79** (2019) 474.
- [63] SINDRUM II collaboration, *A Search for muon to electron conversion in muonic gold*, *Eur. Phys. J. C* **47** (2006) 337.
- [64] DEEME collaboration, *Search for $\mu - e$ conversion with DeeMe experiment at J-PARC MLF*, *PoS FPCP2015* (2015) 060.
- [65] COMET collaboration, *An Overview of the COMET Experiment and its Recent Progress*, in *17th International Workshop on Neutrino Factories and Future Neutrino Facilities*, 12, 2015 [1512.08564].
- [66] COMET collaboration, *COMET Phase-I Technical Design Report*, *PTEP* **2020** (2020) 033C01 [1812.09018].
- [67] COMET collaboration, *Search for Muon-to-Electron Conversion with the COMET Experiment \dagger* , *Universe* **8** (2022) 196 [2203.06365].
- [68] MU2E collaboration, *Mu2e Technical Design Report*, 1501.05241.
- [69] ATLAS collaboration, *Search for the lepton flavor violating decay $Z \rightarrow e\mu$ in pp collisions at \sqrt{s} TeV with the ATLAS detector*, *Phys. Rev. D* **90** (2014) 072010 [1408.5774].
- [70] ATLAS collaboration, *Search for lepton-flavor-violation in Z-boson decays with τ -leptons with the ATLAS detector*, *Phys. Rev. Lett.* **127** (2022) 271801 [2105.12491].
- [71] PARTICLE DATA GROUP collaboration, *Review of Particle Physics*, *PTEP* **2022** (2022) 083C01.

- [72] A. Freitas, *Higher-order electroweak corrections to the partial widths and branching ratios of the Z boson*, *JHEP* **04** (2014) 070 [1401.2447].
- [73] ALEPH, DELPHI, L3, OPAL, SLD, LEP ELECTROWEAK WORKING GROUP, SLD ELECTROWEAK GROUP, SLD HEAVY FLAVOUR GROUP collaboration, *Precision electroweak measurements on the Z resonance*, *Phys. Rept.* **427** (2006) 257 [hep-ex/0509008].
- [74] FCC collaboration, *FCC Physics Opportunities: Future Circular Collider Conceptual Design Report Volume 1*, *Eur. Phys. J. C* **79** (2019) 474.
- [75] FCC collaboration, *FCC-ee: The Lepton Collider: Future Circular Collider Conceptual Design Report Volume 2*, *Eur. Phys. J. ST* **228** (2019) 261.
- [76] J. de Blas et al., *Higgs Boson Studies at Future Particle Colliders*, *JHEP* **01** (2020) 139 [1905.03764].
- [77] I. Esteban, M.C. Gonzalez-Garcia, M. Maltoni, I. Martinez-Soler, J.a.P. Pinheiro and T. Schwetz, *NuFit-6.0: Updated global analysis of three-flavor neutrino oscillations*, 2410.05380.
- [78] N.D. Christensen and C. Duhr, *FeynRules - Feynman rules made easy*, *Comput. Phys. Commun.* **180** (2009) 1614 [0806.4194].
- [79] A. Alloul, N.D. Christensen, C. Degrande, C. Duhr and B. Fuks, *FeynRules 2.0 - A complete toolbox for tree-level phenomenology*, *Comput. Phys. Commun.* **185** (2014) 2250 [1310.1921].